Improved Approximations for Control Augmented Structural Synthesis

H. L. Thomas,* A. E. Sepulveda,† and L. A. Schmit‡
University of California, Los Angeles, Los Angeles, California 90024

A methodology for control augmented structural synthesis is presented for structure-control systems that can be modeled as an assemblage of beams and nonstructural mass elements augmented by a noncollocated direct output feedback control system. Beam cross-sectional dimensions, nonstructural masses and rotary inertias, and controller position and velocity gains are treated simultaneously as design variables. The structural mass or a control system performance index can be minimized with design constraints placed on dynamic harmonic displacements and forces, structural frequencies, and closed-loop eigenvalues and damping ratios. Optimization is carried out by generating and solving a sequence of explicit approximate design problems subject to move limits in the design space. Intermediate design variable and intermediate response quantity concepts are used to enhance the quality of the approximate design problem statements. These concepts are used to generate new approximations for displacements and actuator forces under harmonic dynamic loads and for system complex eigenvalues. This improves the overall efficiency of the integrated design synthesis procedure by reducing the number of complete analyses required for convergence. Numerical results that illustrate the effectiveness of the method presented are given.

Introduction

LARGE space structures, which will be very flexible due to low weight requirements, will need some type of active control system for vibration suppression and to maintain stringent shape specifications.[1,2] Vibrations and shape variations can be induced by positioning maneuvers, motion of mass within the structure, thermal gradients, and docking procedures. Stringent shape specifications are required to maintain pointing accuracy of optical and radar equipment. Because of their size and flexibility, large space structures will have vibrations with low frequencies and long decay times. The low frequency of the structural vibrations may interact with the control system dynamics.

The usual approach to structure-control system synthesis is to first design the structure, with constraints on weight, static and dynamic displacement and stresses, and open-loop eigenvalues (natural frequencies), and then design a control system for this structure, with constraints on the closed-loop eigenvalues (poles), dynamic response, and control forces. If the constraints on the control system design cannot be met, the structure is redesigned and another pass is made at the control system design. Typically this iterative cycling occurs because the structure is designed for low weight and is, therefore, very flexible. Because of this flexibility, excessive control effort is needed. Modifications to the structure can also lead to beneficial changes in the closed-loop eigenvalues. Structural modifications also lead to changes in the control system, especially if linear optimal control theory is used for the control system design.[3-10] Because of the iterative nature of this approach to structure-control system design, with two different sets of objective functions and constraints, convergence to a final design may be slow. Simultaneous synthesis of the structure-control system overcomes the problem of the slow convergence inherent to the iterative approach because there is one set of constraints and the interaction of structural and control system dynamics is taken into account.

This paper describes an efficient and truly simultaneous approach to structure-control system synthesis using an objective function that is either the structural weight or the control system performance and one set of constraints. A high-quality nonlinear, but explicit, approximate design problem is constructed at each stage using analysis results and first-order sensitivity information generated for the current trial design. This approximate optimization problem is then solved to find the next trial design. The generation and solution of approximate design optimization problems is repeated until the sequence of trial designs converges.

There have been various works published on simultaneous structure-control system synthesis.[3-17] In Refs. 3–10, the control gains are treated as dependent design variables and they are determined by use of the Riccati equation. In Refs. 11–17, the control system gains are treated as independent design variables. The approximation concepts approach was first applied to structure-control system synthesis problems in Ref. 15.

In Refs. 15 and 16, a design methodology was developed to synthesize control augmented beam/truss structures by minimizing an objective function consisting of a weighted sum of structural mass, dynamic harmonic response at selected locations, and control forces under dynamic harmonic loading. Constraints were placed on static displacements and stresses, dynamic harmonic response and control force, as well as structural (open-loop) frequencies. This work was extended in Ref. 17 to include noncollocated controllers and constraints on the real and imaginary parts of the closed-loop eigenvalues as well as damping ratios. A description of the simultaneous structure-control system synthesis problem treated here and the optimization methodology employed follows.

Problem Statement

The structure-control system synthesis problem is stated as the following: Seek a design Y^* that minimizes some measure

Presented as Paper 90-1060 at the AIAA/ASME/ASCE/AHS/ASC 31st Structures, Structural Dynamics, and Materials Conference, Long Beach, CA, April 2–4, 1990; received July 27, 1990; revision received Dec. 6, 1990; accepted for publication Jan 22, 1991.

*Graduate Research Assistant, Department of Mechanical, Aerospace and Nuclear Engineering; currently Research Engineer, VMA Engineering, Goleta, CA. Student Member AIAA.

†Postdoctoral Research Associate, Department of Civil Engineering. Member AIAA.

‡Professor of Engineering and Applied Science, School of Engineering and Applied Science. Fellow AIAA.

of system performance subject to constraints on system behavior and bounds on the design variables. This is stated as

Minimize

$$M(\boldsymbol{Y}) \quad \text{or} \quad \sum_j F_j(\boldsymbol{Y}) \tag{1}$$

subject to

$$g_q(\boldsymbol{Y}) \leq 0; \quad q \in Q \tag{2}$$

with bounds

$$Y_n^L \leq Y_n \leq Y_n^U: \quad n \in N \tag{3}$$

The objective function is either the structural mass M or the sum of the amplitudes of the control forces in j control elements F_j. These two quantities are functions of the design variables $\boldsymbol{Y}$, which are beam element cross-sectional dimensions, nonstructural masses and rotary inertias, and control system position and velocity gains. The constrained quantities are dynamic harmonic displacements, control forces caused by dynamic harmonic loads, structural (open-loop) frequencies, closed-loop eigenvalues (both the real and imaginary parts), and damping ratios. In addition, the total structural mass and the total control effort can also be constrained to be below some prescribed values.

Two practical approaches to control agumented structural synthesis are pursued here. The first is to minimize the structural mass with constraints on the total control force (sum of the control force amplitudes) and on the dynamic displacements of nodes at critical locations. The problem is then stated as

Minimize

$$M(\boldsymbol{Y}) \tag{4}$$

subject to $g_q(\boldsymbol{Y}) \leq 0$: $\quad q \in Q$

$$\sum_j F_j(\boldsymbol{Y}) \leq F_T^U \tag{5}$$

with bounds

$$Y_n^L \leq Y_n \leq Y_n^U; \quad n \in N$$

where F_T^U is the upper bound on the total control force, and separate constraints on the dynamic displacements at critical locations are included in g_q.

The other practical approach is to minimize the total control force with constraints on the structural mass and dynamic displacements. This problem is stated as

Minimize

$$\sum_j F_j(\boldsymbol{Y}) \tag{6}$$

subject to $g_q(\boldsymbol{Y}) \leq 0$; $\quad q \in Q$

$$M(\boldsymbol{Y}) \leq M^U \tag{7}$$

with bounds

$$Y_n^L \leq Y_n \leq Y_n^U; \quad n \in N$$

where M^U is the upper bound on the structural mass, and separate constraints on the dynamic displacement at critical locations are included in g_q.

The problem statement defined by Eqs. (4) and (5) leans toward the structural designer's point of view but still takes into account constraints on the control system. The problem statement defined by Eqs. (6) and (7) is more like the approach taken by the control system designer, but it also includes constraints on the structural mass and the structural response.

An efficient approach to design synthesis is to generate and then solve a sequence of approximate optimization problems.[18] At the beginning of each design stage, the structure-control system undergoes full static, dynamic harmonic response, natural frequency, and complex eigenvalue analyses in order to determine the values of the behavior constraints. To lower the computational cost of the sensitivity analysis, the constraints that are not active or potentially active are deleted from the design problem for that stage. Then, first-order analytical sensitivities of appropriate response quantities with respect to the controller gains, nonstructural masses, and beam member section properties are calculated and used to construct an approximate optimization problem. The calculation of sensitivities of response quantities associated with the static, dynamic harmonic response, and the natural frequency analyses are described in Ref. 16. The calculation of sensitivities of the complex eigenvalues is described in Ref. 17.

Each approximate problem in the sequence is then created using the aforementioned sensitivities. These problems are nonlinear but explicit and, therefore, they are very inexpensive to solve compared to the solution of the actual problem. A description of the approximate problem is presented in the next section. Each approximate optimization problem is solved using CONMIN[19] to generate a new design point, which is then analyzed at the beginning of the next stage.

This process is continued until the objective function changes less than some prescribed value for three consecutive stages. The entire synthesis process is summarized in Fig. 1.

Approximate Problem Formulation

In seeking robust approximations of behavior constraints and objective function, it is important to appreciate the flexibility offered by the use of intermediate design variables and intermediate response quantities. These ideas originally introduced in Ref. 18 have recently been applied with considerable success (e.g., see Refs. 20–22), In Ref. 20, it is shown that linear approximations of the natural frequency squared ω^2 with respect to frame member section properties leads to good approximations for natural frequency constraints. In Ref. 21, it is shown that linear approximations of frame member end forces in terms of section properties leads to high-quality static stress approximations. Also in Ref. 22, it is shown that high-quality approximations for natural frequency

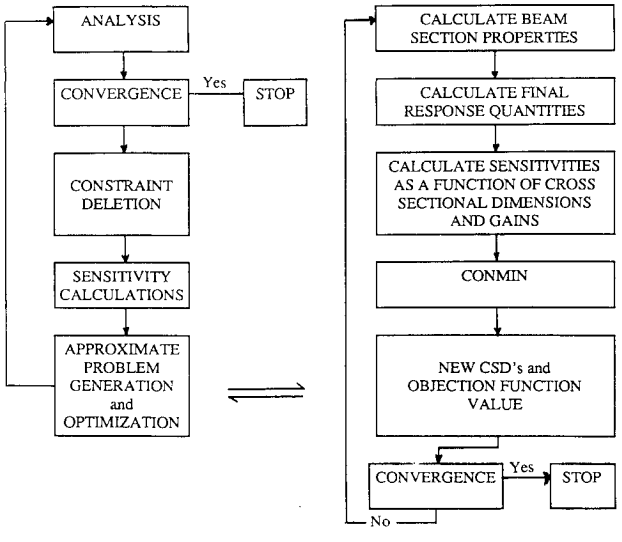

Fig. 1 Optimization procedure.

constraints can be generated by using the Rayleigh quotient expression:

$$\omega_n^2 = \frac{U_n}{T_n} = \frac{\{\phi_n\}^T [K] \{\phi_n\}}{\{\phi_n\}^T [M] \{\phi_n\}} \tag{8}$$

This is done by constructing separate linear approximations for the modal strain energy U_n and the modal kinetic energy T_n, in terms of member section properties, based on assuming invariance of the mode shape vector $\{\phi_n\}$, for moderate design changes (i.e., within move limits selected to protect the approximate representation).

Intermediate Design Variables

In the work reported here, the set of actual design variables ($\boldsymbol{Y}$) that will be treated simultaneously during the optimization is made up of frame member cross-sectional dimensions (CSDs) such as h and b, nonstructural masses and rotary inertias, m, I_m, as well as controller position and velocity gains, h_p and h_v. An examination of the underlying analysis equations reveals that the key matrices involved in both the static and dynamic analyses (i.e., K, M, K_A, C_A, H_p, H_v) are linear functions of all the foregoing design variables except the frame member CSDs. However, these key matrices are linear functions of member direct section properties (DSPs), such as A_f, I_1, I_2, J, and for any particular type of cross section, the DSPs are available as explicit nonlinear functions of the frame member CSDs. Therefore, in the work to be reported here, the set of intermediate design variables making up ($\boldsymbol{X}$) includes A_f, I_1, I_2, J, m, I_m, h_p, and h_v, whereas the set of actual design variables making up ($\boldsymbol{Y}$) includes m, I_m, h_p, and h_v, as well as CSDs such as b and h.

In general, it is to be understood that the intermediate design variables ($\boldsymbol{X}$) must be expressible as explicit functions of the actual design variables, that is, $\boldsymbol{X} = \boldsymbol{X}(\boldsymbol{Y})$. For the particular class of problem studied here, all of the intermediate design variables, except the frame member DSPs (A_f, I_1, I_2, J), are identically equal to an actual design variable ($X_i = Y_i$) and the DSPs can be expressed as explicit functions of the CSDs for any specific type of cross section (for example, $I = bh^3/12$ for a rectangular cross section).

Intermediate Response Quantities

It is often the case that the behavior constraints g_q and the objective function used to describe a design optimization problem can be written as explicit nonlinear functions of intermediate response quantities ($\boldsymbol{R}$), intermediate design variables ($\boldsymbol{X}$), and actual design variables ($\boldsymbol{Y}$). In general, the foregoing statement can be expressed as follows,

$$g_q(\boldsymbol{R},\boldsymbol{X},\boldsymbol{Y}) \leq 0 \tag{9}$$

To fix ideas, consider the following simple example for a static stress constraint in a beam

$$g_q = \frac{P}{A_f} + \frac{M(h/2)}{I} - \sigma_{\text{allow}} \leq 0 \tag{10}$$

Where P and M are intermediate response quantities ($\boldsymbol{R}$), A_f and I are intermediate design variables ($\boldsymbol{X}$), and h is an actual design variable in ($\boldsymbol{Y}$). In this work, it is assumed that all intermediate response quantities ($\boldsymbol{R}$) are implicit functions of the intermediate design variables ($\boldsymbol{X}$) represented by a computer program, which given ($\boldsymbol{X}_o$) generates $\boldsymbol{R}(\boldsymbol{X}_o)$ and $\partial\boldsymbol{R}(\boldsymbol{X}_o)\partial\boldsymbol{X}_i$. These function values and first derivatives of $\boldsymbol{R}$, evaluated at ($\boldsymbol{X}_o$), can then be used to form an explicit approximate relationship between the intermediate response quantities ($\boldsymbol{R}$) and the intermediate design variables ($\boldsymbol{X}$). For example,

$$\boldsymbol{R} \approx \tilde{\boldsymbol{R}} = \boldsymbol{R}(\boldsymbol{X}_o) + \sum_i (X_i - X_{oi}) \frac{\partial \boldsymbol{R}(\boldsymbol{X}_o)}{\partial X_i} \tag{11}$$

or alternatively reciprocal variable or hybrid approximations[23] for the components of $\boldsymbol{R}$ can be constructed using the numerical information contained in $\boldsymbol{R}(\boldsymbol{X}_o)$ and $\partial\boldsymbol{R}(\boldsymbol{X}_o)/\partial X_i$. Now, if $\boldsymbol{R}$ is replaced by $\tilde{\boldsymbol{R}}$ in Eq. (9), an explicit approximation for $g_q(\boldsymbol{Y})$ as a function of the actual design variables ($\boldsymbol{Y}$) emerges, that is,

$$g_q(\boldsymbol{Y}) \approx \tilde{g}_q(\boldsymbol{Y}) = \tilde{g}_q(\tilde{\boldsymbol{R}},\boldsymbol{X},\boldsymbol{Y}) \leq 0 \tag{12}$$

It must be emphasized that in the foregoing equation $\tilde{g}_q(\tilde{\boldsymbol{R}},\boldsymbol{X},\boldsymbol{Y})$ is an explicit function of $\tilde{\boldsymbol{R}}$, $\boldsymbol{X}$, and $\boldsymbol{Y}$; $\tilde{\boldsymbol{R}}$ is an explicit function of $\boldsymbol{X}$; and $\boldsymbol{X}$ is an explicit function of $\boldsymbol{Y}$. During the solution of each approximate optimization problem, constraint function values are evaluated from the explicit functions $\tilde{g}_q(\boldsymbol{Y})$ and the derivatives $\partial\tilde{g}_q(\boldsymbol{Y})/\partial Y_j$ are also evaluated from explicit functions obtained by chain rule differentiation, that is,

$$\frac{\partial \tilde{g}_q(\boldsymbol{Y})}{\partial Y_j} = \sum_k \sum_i \frac{\partial \tilde{g}_q}{\partial \tilde{R}_k} \left(\frac{\partial \tilde{R}_k}{\partial X_i} \right) \frac{\partial X_i}{\partial Y_j} + \sum_i \frac{\partial \tilde{g}_q}{\partial X_i} \frac{\partial X_i}{\partial Y_j} + \frac{\partial \tilde{g}_q}{\partial Y_j} \tag{13}$$

where $\partial\tilde{R}_k/\partial X_i = \partial R_k(\boldsymbol{X}_o)/\partial X_i$ are numerical quantities and all other derivatives are calculated from explicit functions.

With this general background in place, attention is now directed to specific intermediate response quantities used in the work reported here. In the dynamic response analysis, the sine and cosine components of the actuator forces F_s and F_c as well as the real and imaginary components of the dynamic displacements c_R and c_I are taken as intermediate response quantities in ($\boldsymbol{R}$). The explicit approximations of these intermediate response quantities (F_s, F_c, c_R, c_I) in terms of intermediate design variables $\boldsymbol{X}$ can be linear [see Eq. (11)], reciprocal, or hybrid at the users option. The amplitude of the actuator force is approximated by

$$F \approx \tilde{F} = \sqrt{\tilde{F}_s^2 + \tilde{F}_c^2} \tag{14}$$

and the amplitude of the dynamic displacement can be approximated by

$$u_D \approx \tilde{u}_D = \sqrt{\tilde{c}_R^2 + \tilde{c}_I^2} \tag{15}$$

It should be emphasized that the use of appropriate intermediate response quantities captures the explicit nonlinearity inherent to the definition of force and displacement amplitude.

In the case of natural frequencies, the modal strain energy U_n and modal kinetic energy T_n are taken as the intermediate response quantities in ($\boldsymbol{R}$). As in the foregoing discussion, the explicit approximations of these intermediate response quantities, in terms of intermediate design variables ($\boldsymbol{X}$), can be linear, reciprocal, or hybrid. However, since $[K]$ and $[M]$ are linear functions of the intermediate design variables ($\boldsymbol{X}$) for the class of problems treated here, linear approximations for $\tilde{U}_n$ and $\tilde{T}_n$ are the preferred option, assuming the mode shape vectors can be held invariant. The square of the natural frequency for mode n is approximated as

$$\omega^2 = \tilde{\omega}_n^2 = \frac{\tilde{U}_n}{\tilde{T}_n} = \frac{\{\phi_n\}^T [\tilde{K}] \{\phi_n\}}{\{\phi_n\}^T [\tilde{M}] \{\phi_n\}} \tag{16}$$

The equations of motion governing the dynamic behavior of the control augmented structures considered here can be written as follows,

$$[M]\{\ddot{u}\} + [C_A]\{\dot{u}\} + [K_A + i\gamma K]\{u\} = \{P\} \tag{17}$$

where $[C_A] = [C] + [H_v]$ denotes the control augmented damping matrix, $[K_A] = [K] + [H_p]$ denotes the control augmented stiffness matrix, and $[i\gamma K]$ represents preassigned structural damping. Since noncollocated actuator-sensor pairs

are considered, the matrics $[C_A]$ and $[K_A]$ are not symmetric. Defining the state-space variables as

$$\{q\} = \begin{Bmatrix} \dot{u} \\ u \end{Bmatrix} \tag{18}$$

letting $\{P\} = \{0\}$ in Eq. (17) and combining the identity $[M]\{\dot{u}\} - [M]\{\dot{u}\} = \{0\}$ with Eq. (17) leads to the equations of motion in first-order form, namely,

$$[M^*]\{\dot{q}\} + [K^*]\{q\} = \{0\} \tag{19}$$

where

$$[M^*] = \begin{bmatrix} [0] & [M] \\ [M] & [C_A] \end{bmatrix} \tag{20a}$$

$$[K^*] = \begin{bmatrix} -[M] & [0] \\ [0] & [K_A] + i\gamma[K] \end{bmatrix} \tag{20b}$$

Assuming solutions of Eq. (19) having the general form $q = \{\phi\} e^{\lambda t}$ leads to the complex eigenproblem

$$(\lambda[M^*] + [K^*])\{\phi\}_R = \{0\} \tag{21}$$

and the corresponding adjoint problem

$$\{\phi\}_L^T (\lambda[M^*] + [K^*]) = \{0\}^T \tag{22}$$

Premultiplying Eq. (21) by $\{\phi\}_L^T$ or postmultiplying Eq. (22) by $\{\phi\}_R$ and solving for λ gives

$$\lambda = -\frac{\{\phi\}_L^T [K^*] \{\phi\}_R}{\{\phi\}_L^T [M^*] \{\phi\}_R} = -\frac{U^*}{T^*} = -\frac{(U_r^* + iU_i^*)}{(T_r^* + iT_i^*)} \tag{23}$$

where U^* and T^* are thought of as complex pseudomodal energies. The use of modal energies as intermediate response quantities can be extended to the task of generating high-quality approximations for the complex eigenvalues. One approach would be to form the approximation as

$$\tilde{\lambda} = \tilde{\sigma} + i\tilde{\omega}_d = -\frac{\tilde{U}^*}{\tilde{T}^*} = -\frac{\tilde{U}_r^* + i\tilde{U}_i^*}{\tilde{T}_r^* + i\tilde{T}_i^*} \tag{24}$$

assuming the eigenvectors $\{\phi\}_L$ and $\{\phi\}_R$ are invariant for moderate changes in the design. However, the right and left eigenvectors $\{\phi\}_R$ and $\{\phi\}_L$ are, in general, complex and they have the form

$$\{\phi\} = \begin{Bmatrix} \{\phi_v\} \\ \{\phi_p\} \end{Bmatrix} = \begin{Bmatrix} \lambda\{\phi_p\} \\ \{\phi_p\} \end{Bmatrix} \tag{25}$$

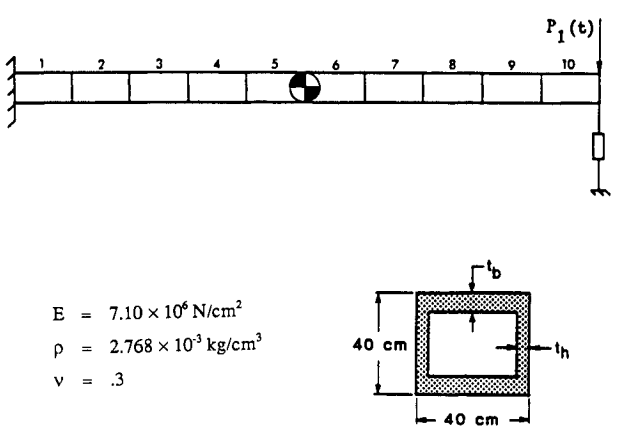

Fig. 2 Cantilevered beam, problem 1.

where $\{\phi_p\}$ is the mode shape associated with position and $\{\phi_v\}$ is the mode shape associated with velocity. It is observed in Eq. (25) that the eigenvector is, in general, not invariant with changes in the eigenvalue.

A better formulation for the approximation of complex eigenvalues is generated by looking at the second-order eigenproblem

$$\lambda^2[M]\{\phi_p\}_R + \lambda[C_A]\{\phi_p\}_R + ([K_A] + i\gamma[K])\{\phi_p\}_R = 0 \tag{26}$$

Premultiplying by $\{\phi_p\}_L^T$ and solving for λ gives

$$\lambda = \sigma + i\,\omega_d = \frac{-S^{\wedge} \pm [(S^{\wedge})^2 - 4U^{\wedge}T^{\wedge}]^{\frac{1}{2}}}{2T^{\wedge}} \tag{27}$$

where

$$U^{\wedge} = \{\phi_p\}_L^T ([K_A] + i\gamma[K])\{\phi_p\}_R = U_r^{\wedge} + iU_i^{\wedge} \tag{28a}$$

$$T^{\wedge} = \{\phi_p\}_L^T [M]\{\phi_p\}_R = T_r^{\wedge} + iT_i^{\wedge} \tag{28b}$$

$$S^{\wedge} = \{\phi_p\}_L^T [C_A]\{\phi_p\}_R = S_r^{\wedge} + iS_i^{\wedge} \tag{28c}$$

Selecting the + sign option in Eq. (27), so that $\omega_d \to \omega > 0$ in the undamped case, substituting Eqs. (28a–c) into Eq. (27) and multiplying the numerator and denominator by $(T_r^{\wedge} - iT_i^{\wedge})$, it can be shown that

$$\sigma = \frac{T_r^{\wedge}(-S_r^{\wedge} + \alpha) + T_i^{\wedge}(-S_i^{\wedge} + \beta)}{2[(T_r^{\wedge})^2 + (T_i^{\wedge})^2]} \tag{29}$$

$$\omega_d = \frac{T_r^{\wedge}(-S_i^{\wedge} + \beta) - T_i^{\wedge}(-S_r^{\wedge} + \alpha)}{2[(T_r^{\wedge})^2 + (T_i^{\wedge})^2]} \tag{30}$$

where α and β are real and can be expressed explicitly in terms of $U_r^{\wedge}$, $U_i^{\wedge}$, $T_r^{\wedge}$, $T_i^{\wedge}$, $S_r^{\wedge}$, and $S_i^{\wedge}$. High-quality approximations $\tilde{\sigma}$ and $\tilde{\omega}_d$ are now formed by constructing explicit approximations for the intermediate response quantities $(\tilde{U}_r^{\wedge}, \tilde{U}_i^{\wedge}, \tilde{S}_r^{\wedge}, \tilde{S}_i^{\wedge}, \tilde{T}_r^{\wedge}, \tilde{T}_i^{\wedge})$ and substituting them into Eqs. (29) and (30), respectively. Furthermore, the damping ratio approximation can be formed using $\tilde{\sigma}$ and $\tilde{\omega}_d$, that is,

$$\xi = \frac{-\tilde{\sigma}}{\sqrt{\tilde{\sigma}^2 + \tilde{\omega}_d^2}} \tag{31}$$

Finally, it is noted that, in the limiting case where all damping vanishes, it can be shown that Eqs. (29) and (30) reduce to $\sigma = 0$ and $\omega_d = \sqrt{U_r/T_r}$.

Examples

The effect of using intermediate design variables and intermediate response quantities on the quality of the approximate problem is shown in the following examples. A more extensive body of computational experience is presented in Ref. 24. The first example problem involves the synthesis of a control augmented cantilever beam and is taken from Ref. 15. The second example problem involves the Draper/Rocket Propulsion Laboratory (RPL) structure and is taken from Ref. 17.

Problem 1—Cantilever Beam: Mass Minimization

The first problem is that of finding the minimum mass design of the 10-m cantilevered beam shown in Fig. 2. The beam is modeled with 10 equal length beam type finite elements. The beam is constrained so that only in-plane vertical motion is followed. A concentrated mass of 200 kg is located at the midspan of the beam. The beam is loaded by a vertical harmonic load of 4000 N at 3.9 Hz applied at the tip; 2% structural damping is assumed. The design variables for this problem are the web and flange thicknesses t_h, t_b of the beam

Table 1 Final designs for problem 1—cantilevered beam: mass minimization

Element type	Element number	Design variables	Final design		
			Uncontrolled	Controlled	Controlled stability constraint
Frame	1–10	t_b, cm	1.995	1.588	1.617
		t_h, cm	0.500[a]	0.500[a]	0.500[a]
Control	1	h_p, N/cm		100.324	86.48
		h_v, N-s/cm		0.217	2.067
Mass, kg			541.4	453.5	459.8

[a]Lower bound value.

Table 2 Final design response ratios for problem 1—cantilevered beam: mass minimization

Constraint	Response ratio		
	Uncontrolled	Controlled	Controlled stability constraints
Tip displacement	1.00[a]	0.996[a]	0.998[a]
Frequency	0.653	0.705	0.700
Control force		1.001[a]	1.000[a]
Stability			0.999[a]

[a]Critical constraint.

elements and the position and velocity gains of a single collocated control element located at the tip of the beam (see Fig. 2).

In this example problem, the web and flange thickness variables are linked along the entire length of the beam. The initial value of the beam element design variables are taken as 5.0 cm with side constraints imposed so that 0.5 cm $\leq t_h$, $t_b \leq 10.0$ cm. The magnitude of the tip displacement of the beam is constrained to be ≤ 10.0 cm, and the first frequency is constrained to be ≥ 4.0 Hz. Move limits of 60% are imposed on the design variables during each stage with a minimum move limit of 0.1.

Three runs are made for this example problem, all starting from the same initial structural design. In the first run, no control elements are used. In the second run, an axial controller is located at the tip of the beam in order to control the vertical displacement at the tip. The initial values of the position and velocity gain design variables in the second and third runs are $h_p = 20.0$ N/cm and $h_v = 2.0$ N-s/cm. Although there are no constraints placed on the control gains, the magnitude of the control force is constrained to be ≤ 1000 N. The third run is the same as the second except that the real part of the complex eigenvalue (stability measure) of the first mode is constrained to be ≤ -1.0 rad/s.

The final designs and final design response ratios for all three runs are given in Tables 1 and 2. The iteration history plots are shown in Fig. 3. In all three cases, the tip displacement constraint is critical. This is to be expected because the minimization of the mass of the structure results in lower structural stiffness. In the second and third runs, where the controller is used, the control force constraint is also critical. This is because the control force increases as the structural stiffness decreases. Note that the addition of critical actuator force constraints does not slow down the convergence of the synthesis process.

The iteration history of the first run (uncontrolled from Ref. 15) is also shown in Fig. 3. Note the faster convergence rate of the new result reported here. This is due to the increased accuracy of the dynamic displacement constraint that is achieved through the use of approximations of intermediate response quantities.

The position gain is much larger than the velocity gain in the final design of the second run. This is because the frequency of the harmonic load is well below the first mode structural frequency, which results in more stiffness augmentation, rather than damping augmentation. The mass of the final design of the second run is lower than that of the first run because of the stiffness augmentation provided by the controller.

In the final design of the second run, the value of the real part of the complex eigenvalue of the first mode is -0.35 rad/s. The stability constraint in the third run requires almost three times as much damping in this mode [i.e., $\sigma_1 \leq -1.0$ rad/s]. The controller velocity gain for the final design of the third run is much higher than that at the end of the second run due to this increased damping requirement. Because of the constraint on the control force, the position gain is forced to decrease from the value obtained in the second run. This results in an increase in the structural mass due to the loss of stiffness augmentation provided by the controllers. Note that the addition of critical dynamic stability constraints does not slow down the convergence of the synthesis process. This can be attributed to the quality of the improved approximations for complex eigenvalue constraints introduced in this work.

In all three runs, the web thickness takes on its minimum gauge. This is because the flange's stiffness to mass ratio is much higher than that of the web.

Problem 2—Draper/RPL Structure: Control Force Minimization

The Draper/RPL structure consists of a massive central hub surrounded by four flexible appendages that have nonstructural mass attached to their free ends (see Fig. 4 and Ref. 13). The entire structure is free to rotate about the central axis of the hub. Table 3 lists the important parameters. Because of the symmetry of the structure, only half of it needs to be used for analysis purposes. The analysis model is shown

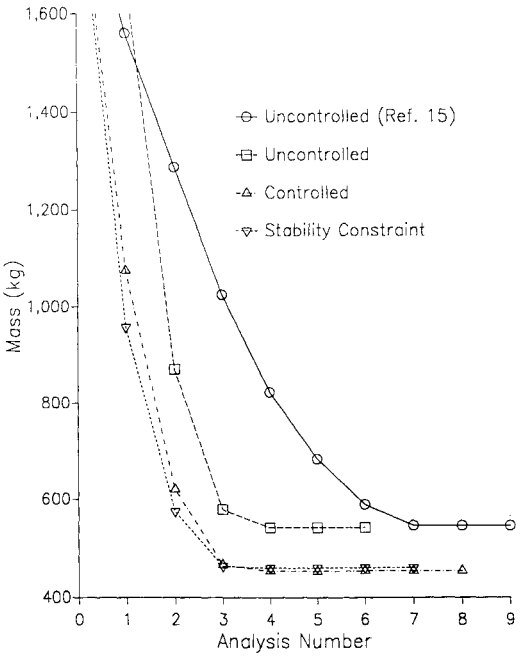

Fig. 3 Iteration histories for problem 1—cantilevered beam: mass minimization.

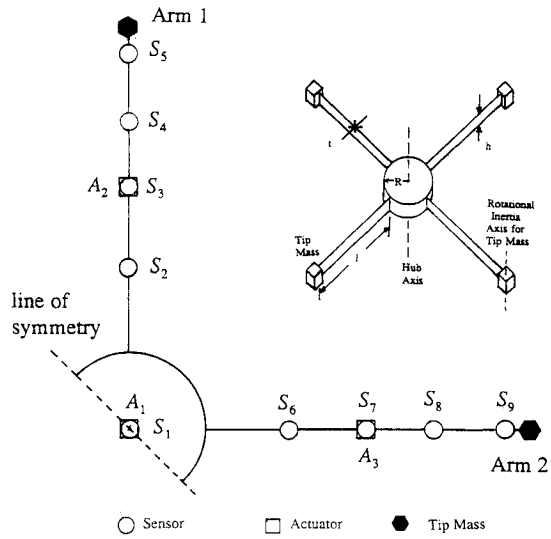

Fig. 4 Draper/RPL structure and analysis model.

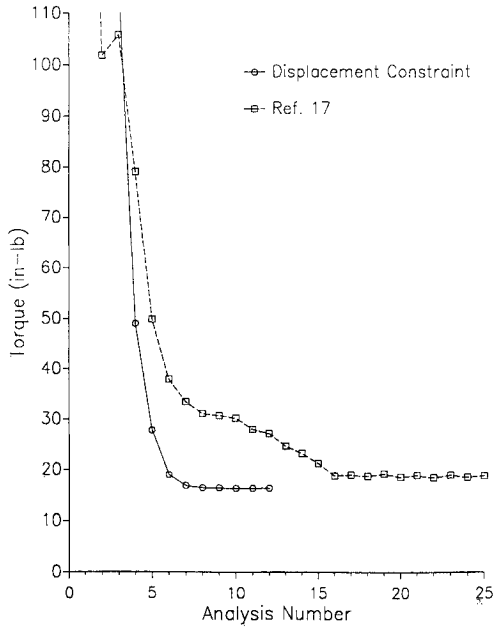

Fig. 5 Iteration history comparison for problem 2—Draper/RPL structure: control force minimization.

in Fig. 4. There are four sensors on each arm at radial positions of r = 24 in. for sensors 2 and 6, r = 36 in. for sensors 3 and 7, r = 43.6 in. for sensors 4 and 8, and r = 55.2 in. for sensors 5 and 9. These sensors measure displacement and velocity in the circumferential direction. There is an additional rotational position and velocity sensor located at the axis of the hub. There are three actuators that apply torques to the structure. Actuator 1 is located at the axis of the hub and actuators 2 and 3 are located at r = 36 in. on arms 1 and 2, respectively. Twenty-one controllers, with sensor-actuator pairs defined in Table 4, will be used to control the structure. The controller and actuator configuration is the same on opposing arms. This actuator-sensor configuration is the same as that used in Ref. 13. Each arm of the structure is modeled with five beam type finite elements. The finite element nodes are located at the edge of the hub, at each sensor location, and at the tip mass.

The first nine open-loop frequencies of the structure, based on a finite element method analysis with 25 DOF, are shown in Table 5. The first frequency corresponds to a rigid-body mode of the structure rotating about its hub axis. Note that the next eight frequencies occur in four closely spaced pairs.

The structure is loaded by a 720.0 in.-lb torque at 3.0 Hz applied at the hub axis of the structure. Structural damping of 0.1% is assumed. The total control force is the objective to be minimized. The design variables are the 42 position and velocity gains. The initial values for the gains are h_p = 10.0 lb-in./rad and h_v = 1.0 lb-in.-s/rad for the controller 1 and h_p = 1.0 lb and h_v = 1.0 lb-s for controllers 2–21. The initial gain values were chosen so that the system had no zero frequency closed-loop modes.

In this example, the total control force is minmized subject to constraints on the complex eigenvalues of the first nine modes and a tip displacement constraint. The damped frequency of mode 1 is constrained to be above 0.3 Hz and the damping ratios for the first nine modes are constrained as the following: above 0.03 for modes 1–3, above 0.01 for modes 4 and 5, above 0.002 for modes 6 and 7, and above 0.0015 for modes 8 and 9. These are the same damping ratio constraints as those used in Ref. 13. The tip displacement of arm 2 is constrained to be $\leq$ 0.1 in. The final design control element forces and final design response ratio values are shown in Tables 6 and 7. The iteration history plot is shown in Fig. 5.

At the final design, five of the nine damping ratio constraints are critical. The control force of many of the control elements is near zero (see Table 6). Control elements 6, 8, 9, and 20 supply most of the control force in the final design. The tip displacement constraint is also critical.

In this problem, because the objective function is total control force, the force and, hence, the gains of the individual control elements are driven toward zero. The control force is a very nonlinear function of the gains when they are near zero. Therefore, the high-quality nonlinear approximation,

Table 3 Draper/RPL dimensions

Hub radius, R	12 in.
Rotary inertia of hub	1152 slug-in.^{2}
Mass density of beams	0.003021 slug/in.^{3}
Elastic modulus of arms	1.1 × 10^7 lb/in.^{3}
Arm thickness, t	0.125 in.
Arm height, h	6.0 in.
Arm length, l	48 in.
Tip mass	0.156941 slug
Rotary inertia of tip mass about its axis	0.2592 slug-in.^{2}
Structural damping	0.1%

Table 4 Draper/RPL structure controller sensor-actuator definitions

	Sensor								
Actuator	1	2	3	4	5	6	7	8	9
1	1	4	—	5	—	2	—	3	—
2	—	18	19	20	21	14	15	16	17
3	—	10	11	13	13	6	7	8	9

Table 5 Draper/RPL structure open-loop frequencies

Mode	Frequency, Hz
1	0.00
2	0.70
3	1.26
4	8.18
5	8.40
6	24.87
7	25.00
8	47.65
9	47.74

Table 6 Final design controller forces for problem 2—Draper/RPL structure: control force minimization

Control element	Controller torque, in.-lb
1	0.005
2	0.005
3	0.005
4	0.006
5	0.003
6	2.555
7	0.082
8	4.300
9	0.399
10	0.052
11	0.006
12	0.007
13	0.001
14	0.004
15	0.005
16	0.002
17	0.014
18	0.004
19	0.012
20	0.739
21	0.003
Total	16.319

Table 7 Final design response ratio values for problem 2—Draper/RPL structure: control force minimization

Constraint	Response ratio
Damped frequency (1)	0.898
Damping ratio (1)	0.769
Damping ratio (2)	0.997[a]
Damping ratio (3)	0.998[a]
Damping ratio (4)	0.997[a]
Damping ratio (5)	0.094
Damping ratio (6)	−4.990
Damping ratio (7)	−28.931
Damping ratio (8)	0.990[a]
Damping ratio (9)	1.000[a]
Tip displacement	0.999[a]

[a]Constraint is critical.

Table 8 Final design response ratios for problem 3—cases A and B grillage

Constraint	Response ratio	
	Case A: control force minimization	Case B: weight minimization
Displacement (joint 1)	1.001[a]	0.996[a]
Displacement (joint 6)	1.001[a]	0.996[a]
Displacement (joint 19)	0.927	1.000[a]
Displacement (joint 24)	0.927	1.000[a]
Stability (mode 1)	0.064	−4.630
Stability (mode 2)	1.000[a]	−5.121
Stability (mode 3)	1.000[a]	0.763
Stability (mode 4)	0.816	0.959
Actuator force (joint 8)	0.261	0.332
Actuator force (joint 11)	0.261	0.332
Actuator force (joint 14)	0.528	0.463
Actuator force (joint 17)	0.528	0.463
Total control force		1.000[a]

[a]Constraint is critical.

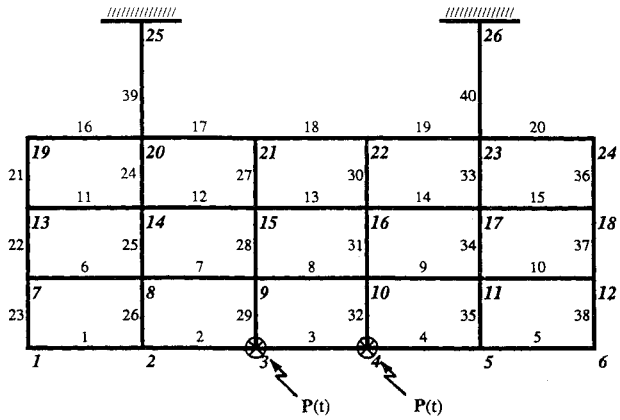

Fig. 6 Grillage, problem 3.

based on the concept of approximate intermediate response quantities, must be used in order to achieve rapid convergence. The effect of this approximation on the convergence rate is shown graphically in Fig. 5. In this plot, the iteration history is shown, for the same problem, prior to the introduction of the refined approximations. The results reported in Ref. 17 were generated without the use of approximations based on intermediate response quantities. Note the oscillation near the optimum. This is caused by the poor quality of the approximations used in Ref. 17. The introduction of refined approximations not only reduces the number of analyses needed for convergence by a factor of 2, but it also leads to an objective function value that is 13.3% lower (16.32 in.-lb compared with 18.82 in.-lb).

Problem 3—Grillage

The final example problem is the design synthesis of the 4 × 6 (72 DOF) control augmented planer grillage shown in Fig. 6. The grillage consists of 10 aluminum frame members (ρ = 0.1 lb/in.^{3}, E = 10.5 × 10^6 lb/in.^{2}, and ν = 0.3) placed on 2-ft centers and cantilevered from two fixed supports by 2-ft-long flexible beams. Each solid rectangular beam is 2.0 in. wide and has an initial thickness of 0.25 in. The members are oriented so that the width dimension lies in the plane of the structure. There are actuators attached to the structure at joints 8, 11, 14, and 17 that act in the z direction. The mass of each actuator (0.5 lbm) is modeled as a fixed nonstructural mass. Sensors, which sense position and velocity in the z direction, are located at joints 1, 6, 19, and 24, as well as 8, 11, 14, and 17. Each actuator is connected to the four corner sensors (at joints 1, 6, 19, and 24) and the sensor at the same joint as the actuator. This results in five sensors per actuator and a total of 40 gain design variables; 2% structural damping is assumed.

The structure is subjected to 5.0-lb loads at 2 Hz at joints 3 and 4 in the z direction. The amplitudes of the dynamic displacements of the corner of the grillage (joints 1, 6, 19, and 24) are constrained to be ≤ 2.0 in. The magnitude of each actuator force is constrained to be ≤ 2.0 lb. Finally, the real part of the complex eigenvalue is constrained to be below −0.05 rad/s for mode 1, −0.10 rad/s for mode 2, −0.20 rad/s for mode 3, and −0.20 rad/s for mode 4. In this problem, move limits of 80% were used during each design stage.

Case A: Control Force Minimization

In this case, the structure is held fixed and the 40 control system gains are the design variables. The initial gains are h_p = 0.0001 lb/in. and h_v = 0.0001 lb-s/in. The final design response ratios and final design control system gains are presented in Tables 8 and 9. The iteration history is plotted in Fig. 7. Note that the total control force is almost zero in the initial design because the control system gains are nearly zero.

Once a near feasible design is achieved (iteration 4), the synthesis problem converges rapidly and monotonically.

Case B: Weight Minimization

This problem is the same as that of case A except that now the beam element thicknesses are also design variables and the weight of the structure is minimized. The total control force is constrained to be less than that of the final design in case A (3.15 lb.). The 10-frame element member thicknesses along with the thickness of the cantilevered supports (elements 39 and 40) make up the 11 structural design variables. This problem has a total of 51 design variables and 13 constraints. The final design response ratios, final design control system variable values, and final design structural variable values are presented in Tables 8, 10, and 11. The iteration history data is plotted in Fig. 7. The final design for this case represents a 37.5% reduction in structural weight from the initial design (30.03 lb as opposed to 48.00 lb). Also note that the two middle horizontal members and the four vertical members that are not connected to the supports achieve the lower bound thickness value (0.1 in.).

Table 9 Final design for problem 3—case A grillage: control force minimization

Sensor joint	Design variables	Actuator joint 8	11	14	17
8	h_p	−0.003			
	h_v	0.000			
11	h_p		−0.003		
	h_v		0.000		
14	h_p			−0.071	
	h_v			0.000	
17	h_p				−0.071
	h_v				0.000
1	h_p	−0.007	−0.007	−0.066	−0.058
	h_v	0.000	0.000	0.003	0.002
6	h_p	−0.007	−0.007	−0.058	−0.066
	h_v	0.000	0.000	0.002	0.003
19	h_p	−0.130	−0.130	−0.158	−0.147
	h_v	0.001	0.000	0.008	0.007
24	h_p	−0.130	−0.130	−0.147	−0.158
	h_v	0.000	0.001	0.007	0.008

Table 10 Control system final design for problem 3—case B grillage: weight minimization

Sensor joint	Design variables	Actuator joint 8	11	14	17
8	h_p	−0.002			
	h_v	0.000			
11	h_p		−0.002		
	h_v		0.000		
14	h_p			0.009	
	h_v			0.000	
17	h_p				0.009
	h_v				0.000
1	h_p	−0.003	−0.003	0.005	0.006
	h_v	0.022	0.005	−0.016	−0.019
6	h_p	−0.003	−0.003	0.006	0.005
	h_v	0.005	−0.022	−0.019	−0.016
19	h_p	−0.002	−0.002	0.005	0.006
	h_v	0.000	0.000	0.000	0.000
24	h_p	−0.002	−0.002	0.006	0.005
	h_v	0.000	0.000	0.000	0.000

Table 11 Structural final design for problem 3—case B grillage: weight minimization

Beam numbers	Thickness, in.
1–5	0.274[a]
6–10	0.100[a]
11–15	0.100[a]
16–20	0.197[a]
21–23	0.100[a]
24–26	0.132[a]
27–29	0.100[a]
30–32	0.100[a]
33–35	0.132[a]
36–38	0.100[a]
39, 40	0.442[a]

[a]At lower bound.

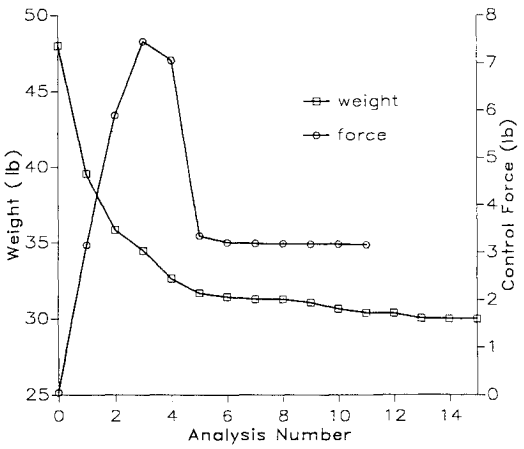

Fig. 7 Iteration history for problem 3—cases A and B grillage.

Conclusions

It has been shown that the introduction of high-quality explicit approximations for behavior constraints on dynamic harmonic displacements and control forces, structural frequencies, closed-loop eigenvalues, and modal damping ratios significantly improves the convergence characteristics of the approximation concepts method when it is extended for application to control augmented structural synthesis problems. It should be noted that noncollocated control configurations and dynamic stability constraints have been considered.

In constructing improved explicit approximations for various behavior constraint functions, the flexibility of intermediate response quantity and intermediate design variable concepts has been exploited. It should be recognized that, in general, each type of behavior constraint can be approximated using different intermediate response quantities and different intermediate design variables, chosen to enhance the quality of approximation. As long as the actual constraints are explicit functions of the intermediate response quantities and the intermediate design variables are explicit functions of the actual design variables, all of the final constraint approximations will be explicit functions of the actual design variables spanning the space where the sequence of approximate design optimization problems is solved. It should also be noted that intermediate design variable and intermediate response quantity concepts can be extended to design problems with transient dynamic loads, especially if the modal method of analysis is used.

Design optimization problems involving a diverse mix of behavior constraints, as well as alternative objective functions, have been solved in a design space that spans structural and control system design variables simultaneously. Convergence to feasible near optimum designs have been obtained after only 6–15 actual analyses, depending on the problem.

Acknowledgment

This research was supported by NASA Research Grant NSG 1490.

References

[1]Nurre, G. S., Ryan, R. S., Scofield, H. N., and Sims, J. L., "Dynamics and Control of Large Space Structures," *Journal of Guidance, Control, and Dynamics*, Vol. 7, No. 5, 1984, pp. 515–526.

[2]Rodriguez, G. (ed.), *Proceedings of the Workshop on Identification and Control of Flexible Space Structures*, Vols. 1–3, Jet Propulsion Laboratory, Pasadena, CA, Publication 85-29, April 1985.

[3]Khot, N. S., Venkayya, V. B., and Eastep, F. E., "Optimal Structural Modifications to Enhance the Active Vibration Control of Flexible Structures," *AIAA Journal*, Vol. 24, No. 8, 1986, pp. 1368–1374.

[4]Khot, N. S., Grandhi, R. V., and Venkayya, V. B., "Structure and Control Optimization of Space Structures," *Proceedings of the AIAA/ASME/ASCE/AHS 28th Structures, Structural Dynamics and Materials Conference*, AIAA, Washington, DC, 1987, pp. 850–860.

[5]Hale, A. L., Lisowski, R. J., and Dahl, W. E., "Optimal Simultaneous Structural and Control Design of Maneuvering Flexible Spacecraft," *Journal of Guidance, Control, and Dynamics*, Vol. 8, No. 1, 1985, pp. 86–93.

[6]Miller, D. F., and Shim, J., "Gradient Based Combined Structural and Control Optimization," *Journal of Guidance, Control and Dynamics*, Vol. 10, No. 3, 1987, pp. 291–298.

[7]Onoda, J., and Haftka, R. T., "An Approach to Structure/Control Stimultaneous Optimization for Large Flexible Spacecraft," *AIAA Journal*, Vol. 25, No. 8, 1987, pp. 1133–1138.

[8]Rao, S. S., Venkayya, V. B., and Khot, N. S., "Game Theory Approach for the Integrated Design of Structures and Controls," *AIAA Journal*, Vol. 26, No. 4, 1988, pp. 463–469.

[9]Belvin, W. K., and Park, K. C., "Structural Tailoring and Feedback Control Synthesis: An Interdisciplinary Approach," *Proceedings of the AIAA/ASME/ASCE/AHS 29th Structures, Structural Dynamics and Materials Conference*, AIAA, Washington, DC, 1988, pp. 1–8.

[10]Messac, A., and Turner, J., "Dual Structural-Control Optimization of Large Space Structures," *Proceedings of the NASA Symposium on Recent Advances in Multidisciplinary Analysis and Optimization*, Part 2, Hampton, VA, April 24–26, 1984, pp. 775–802.

[11]Haftka, R. T., Martinovic, Z. N., and Hallauer, W. L., Jr., "Enhanced Vibration Controllability by Minor Structural Modification," *AIAA Journal*, Vol. 23, No. 8, 1985, pp. 1260–1266.

[12]Khot, N. S., Öz, H., Grandhi, R. V., Eastep, F. E., and Venkayya, V. B., "Optimal Structural Design With Control Gain Norm Constraint," *AIAA Journal*, Vol. 26, No. 5, 1988, pp. 604–611.

[13]Bodden, D. S., and Junkins, J. L., "Eigenvalue Optimization Algorithms for Structure/Controller Design Iterations," *Journal of Guidance, Control, and Dynamics*, Vol. 8, No. 6, 1985, pp. 697–706.

[14]Onoda, V., and Watanabe, N., "Integrated Direct Optimization of Structural/Regulator/Observer for Large Flexible Spacecraft," *Proceedings of the AIAA/ASME/ASCE/AHS/ASE 30th Structures, Structural Dynamics and Materials Conference*, AIAA, Washington, DC, 1989, pp. 1336–1344.

[15]Lust, R. V., and Schmit, L. A., "Control-Augmented Structural Synthesis," *AIAA Journal,* Vol. 26, No. 1, 1988, pp. 86–94.

[16]Lust, R. V., and Schmit, L. A., "Control Augmented Structural Synthesis," NASA CR-4132, April 1988.

[17]Thomas, H. L., and Schmit, L. A., "Control Augmented Structural Synthesis with Dynamic Stability Constraints," *Proceedings of the AIAA/ASME/ASCE/AHS/ASE 30th Structures, Structural Dynamics and Materials Conference*, AIAA, Washington, DC, April 1989, pp. 521–531.

[18]Schmit, L. A., and Miura, H., "Approximation Concepts for Efficient Structural Synthesis," NASA CR 2552, March 1976.

[19]Vanderplaats, G. N., "CONMIN—A Fortran Program for Constrained Function Minimizaion," NASA TM X-62,682, Aug. 1973.

[20]Vanderplaats, G. N., and Salajegheh, E., "An Efficient Approximation Technique for Frequency Constraints in Frame Optimization," *International Journal for Numerical Methods*, Vol. 26, No. 5, 1988, pp. 1057–1069.

[21]Vanderplaats, G. N., and Salajegheh, E., "A New Approximation Method for Stress Constraints in Structural Synthesis," *AIAA Journal*, Vol. 27, No. 3, 1989, pp. 352–358.

[22]Canfield, R. A., "An Approximation Function for Frequency Constrained Structural Optimization," *Proceedings of the NASA Symposium on Recent Advances in Multidisciplinary Analysis and Optimization*, Part 2, Hampton, VA, Sept. 28–30, 1988, pp. 937–953.

[23]Starnes, J. R., Jr., and Haftka, R. T., "Preliminary Design of Composite Wings for Buckling, Stress and Displacement Constraints," *Journal of Aircraft*, Vol. 16, No. 8, 1979, pp. 564–570.

[24]Thomas, H. L., "Improved Approximations for Control Augmented Structural Synthesis, Ph.D. Dissertation, University of California, Los Angeles, CA, 1990.